Time-frequency methods for coherent spectroscopy

Andrea Volpato and Elisabetta Collini*

Dept. of Chemical Sciences, University of Padova, via Marzolo 1, 35131 Padova, Italy
*elisabetta.collini@unipd.it

Abstract: Time-frequency decomposition techniques, borrowed from the signal-processing field, have been adapted and applied to the analysis of 2D oscillating signals. While the Fourier-analysis techniques available so far are able to interpret the information content of the oscillating signal only in terms of its frequency components, the time-frequency transforms (TFT) proposed in this work can instead provide simultaneously frequency and time resolution, unveiling the dynamics of the relevant beating components, and supplying a valuable help in their interpretation. In order to fully exploit the potentiality of this method, several TFTs have been tested in the analysis of sample 2D data. Possible artifacts and sources of misinterpretation have been identified and discussed.

OCIS codes: (070.0070) Fourier optics and signal processing; (300.6300) Spectroscopy, Fourier transforms; (300.6500) Spectroscopy, time-resolved; (270.0270) Quantum optics; (200.4560) Optical data processing; (030.1670) Coherent optical effects.

References and links

1. S. Mukamel, *Principles of Nonlinear Optics and Spectroscopy* (Oxford University, 1995).
2. E. Collini, "Spectroscopic signatures of quantum-coherent energy transfer," Chem. Soc. Rev. **42**(12), 4932–4947 (2013).
3. Y.-C. Cheng and G. R. Fleming, "Coherence quantum beats in two-dimensional electronic spectroscopy," J. Phys. Chem. A **112**(18), 4254–4260 (2008).
4. A. Halpin, P. J. M. Johnson, R. Tempelaar, R. S. Murphy, J. Knoester, T. L. C. Jansen, and R. J. D. Miller, "Two-dimensional spectroscopy of a molecular dimer unveils the effects of vibronic coupling on exciton coherences," Nat. Chem. **6**(3), 196–201 (2014).
5. E. Collini and G. D. Scholes, "Coherent intrachain energy migration in a conjugated polymer at room temperature," Science **323**(5912), 369–373 (2009).
6. E. Collini, C. Y. Wong, K. E. Wilk, P. M. G. Curmi, P. Brumer, and G. D. Scholes, "Coherently wired light-harvesting in photosynthetic marine algae at ambient temperature," Nature **463**(7281), 644–647 (2010).
7. E. Romero, R. Augulis, V. I. Novoderezhkin, M. Ferretti, J. Thieme, D. Zigmantas, and R. van Grondelle, "Quantum coherence in photosynthesis for efficient solar-energy conversion," Nat. Phys. **10**(9), 676–682 (2014).
8. Y. Song, S. N. Clafton, R. D. Pensack, T. W. Kee, and G. D. Scholes, "Vibrational coherence probes the mechanism of ultrafast electron transfer in polymer-fullerene blends," Nat. Commun. **5**, 4933 (2014).
9. V. Tiwari, W. K. Peters, and D. M. Jonas, "Electronic resonance with anticorrelated pigment vibrations drives photosynthetic energy transfer outside the adiabatic framework," Proc. Natl. Acad. Sci. USA **110**(4), 1203–1208 (2013).
10. S. F. Huelga and M. B. Plenio, "Vibrations, quanta and biology," Contemp. Phys. **54**(4), 181–207 (2013).
11. A. Kolli, E. J. O'Reilly, G. D. Scholes, and A. Olaya-Castro, "The fundamental role of quantized vibrations in coherent light harvesting by cryptophyte algae," J. Chem. Phys. **137**(17), 174109 (2012).
12. G. S. Engel, T. R. Calhoun, E. L. Read, T.-K. Ahn, T. Mancal, Y.-C. Cheng, R. E. Blankenship, and G. R. Fleming, "Evidence for wavelike energy transfer through quantum coherence in photosynthetic systems," Nature **446**(7137), 782–786 (2007).
13. N. Christensson, H. F. Kauffmann, T. Pullerits, and T. Mančal, "Origin of long-lived coherences in light-harvesting complexes," J. Phys. Chem. B **116**(25), 7449–7454 (2012).
14. A. W. Chin, J. Prior, R. Rosenbach, F. Caycedo-Soler, S. F. Huelga, and M. B. Plenio, "The role of non-equilibrium vibrational structures in electronic coherence and recoherence in pigment-protein complexes," Nat. Phys. **9**(2), 113–118 (2013).
15. X. Wu and T. Liu, "Spectral decomposition of seismic data with reassigned smoothed pseudo Wigner–Ville distribution," J. Appl. Geophys. **68**(3), 386–393 (2009).

#240965 Received 14 May 2015; revised 23 Jun 2015; accepted 26 Jun 2015; published 17 Jul 2015

16. E. Pereira de Souza Neto, M.-A. Custaud, J. Frutoso, L. Somody, C. Gharib, and J.-O. Fortrat, "Smoothed pseudo Wigner-Ville distribution as an alternative to Fourier transform in rats," Auton. Neurosci. **87**(2-3), 258–267 (2001).
17. K. Gröchenig, *Foundations of Time-Frequency Analysis* (Springer Science, 2001).
18. T. Jo Lynn and A. Z. Bin Sha'ameri, "Signal analysis and classification of digital communication signals using adaptive smooth-windowed Wigner-Ville distribution," in *Proceedings of IEEE Conference on Telecommunication Technologies* (IEEE, 2008), pp. 260–266.
19. M. J. J. Vrakking, D. M. Villeneuve, and A. Stolow, "Observation of fractional revivals of a molecular wave packet," Phys. Rev. A **54**(1), R37–R40 (1996).
20. T. Fuji, T. Saito, and T. Kobayashi, "Dynamical observation of Duschinsky rotation by sub-5-fs real-time spectroscopy," Chem. Phys. Lett. **332**(3-4), 324–330 (2000).
21. D. Hasegawa, K. Nakata, E. Tokunaga, K. Okamura, J. Du, and T. Kobayashi, "Vibrational energy flow between modes by dynamic mode coupling in THIATS J-aggregates," J. Phys. Chem. A **117**(45), 11441–11448 (2013).
22. T. Kobayashi and A. Yabushita, "Transition-state spectroscopy using ultrashort laser pulses," Chem. Rec. **11**(2), 99–116 (2011).
23. A. Yabushita and T. Kobayashi, "Primary conformation change in bacteriorhodopsin on photoexcitation," Biophys. J. **96**(4), 1447–1461 (2009).
24. S. M. Kay, *Modern Spectral Estimation: Theory and Application* (Prentice Hall, 1988).
25. S. L. Marple, *Digital Spectral Analysis: With Applications* (Prentice Hall, 1987).
26. L. Cohen, "Generalized phase-space distribution functions," J. Math. Phys. **7**(5), 781–786 (1966).
27. C. H. Page, "Instantaneous power spectra," J. Appl. Phys. **23**(1), 103–106 (1952).
28. A. W. Rihaczek, "Signal energy distribution in time and frequency," IEEE Trans. Inf. Theory **14**(3), 369–374 (1968).
29. Y. Zhao, L. E. Atlas, and R. J. Marks II, "The use of cone-shaped kernels for generalized time-frequency representations of nonstationary signals," IEEE Trans. Acoust. Speech **38**(7), 1084–1091 (1990).
30. D. Gabor, "Theory of communication," J. of IEEE **93**, 429–457 (1943).
31. J. Prior, E. Castro, A. W. Chin, J. Almeida, S. F. Huelga, and M. B. Plenio, "Wavelet analysis of molecular dynamics: efficient extraction of time-frequency information in ultrafast optical processes," J. Chem. Phys. **139**(22), 224103 (2013).
32. R. D. Hippenstiel and P. M. de Oliveira, "Time-varying spectral estimation using the instantaneous power spectrum (IPS)," IEEE Trans. Acoust. Speech **38**(10), 1752–1759 (1990).
33. H. Margenau and R. N. Hill, "Correlation between measurements in quantum theory," Prog. Theor. Phys. **26**(5), 722–738 (1961).
34. E. Wigner, "On the quantum correction for thermodynamic equilibrium," Phys. Rev. **40**(5), 749–759 (1932).
35. J. Ville, "Théorie et application de la notion de signal analytique," Câbles et Transmissions **2eA**, 61–74 (1948).
36. L. Cohen, "Time-frequency distributions-a review," Proc. IEEE **77**(7), 941–981 (1989).
37. T. A. C. M. Claasen and W. F. G. Mecklenbrauker, "Wigner distribution - A tool for time-frequency signal analysis," Philips J. Res. **35**, 217–250 (1980).
38. H. I. Choi and W. J. Williams, "Improved time-frequency representation of multicomponent signals using exponential kernels," IEEE Trans. Acoust. Speech **37**(6), 862–871 (1989).
39. S. Qian and C. Dapang, "Joint time-frequency analysis," IEEE Signal Process. Mag. **16**(2), 52–67 (1999).

1. Introduction

Femtosecond coherence spectroscopy is a family of ultrafast techniques that utilize ultrafast laser pulses to prepare and monitor coherent states in resonant or nonresonant samples [1]. The evolution of a coherent superposition of states is manifested in the experimental signals as oscillations in the amplitude as a function of time [2, 3]. Among coherence spectroscopies, 2D electronic spectroscopy (2DES) techniques have recently gained particular interest given their capability of following ultrafast energy transport processes in real time. In the last decade indeed several 2DES studies reported about coherent dynamics in biological and artificial light-harvesting systems [4–8]. In many of these systems the physical origin as well as the possible functional role of these coherent dynamics in the energy or charge transfer processes is still being intensively debated [9–11].

While such oscillations were indeed initially attributed to excitonic beatings and associated with quantum transport [5, 6, 12], more recent theoretical and experimental investigations recognized a more complex nature of the 2D signal oscillations, whose origin often cannot be unambiguously determined. In general, both vibrational and electronic coherence effects may contribute to the appearance of beating in the spectroscopic signals, since ultrafast pulses may excite superpositions of electronic as well as vibrational states [9, 11, 13, 14].

#240965 Received 14 May 2015; revised 23 Jun 2015; accepted 26 Jun 2015; published 17 Jul 2015

It is thus necessary to set up new tools to characterize and analyze these coherence signals with greater depth and accuracy. The analysis of the oscillations bringing the information on coherent dynamics can be indeed quite puzzling, since typically they are the results of the superposition of several beating components, each of which is characterized by different frequencies and time-dependent amplitudes [Fig. 1]. This is what is generally defined as multi-component non-stationary oscillatory behavior. In order to assess the nature of the different components, one must extract from the overall signal not only the frequency of the different components, associated with the energy of the states involved in the coherent superposition, but also their time behavior, whose knowledge may represent a valuable help in the assessment of their nature.

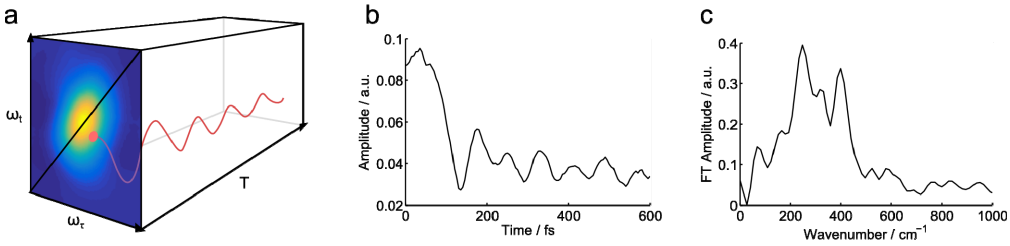

Fig. 1. (a) Pictorial representation of the 3D data set typically obtained with a 2DES experiment; the evolution of a 2D frequency-frequency map is measured along the delay time T. (b) The decay of the signal can be extracted at a given coordinate on the frequency-frequency map as a function of the delay time T. The obtained oscillating trace has the same typical behavior of oscillating signals obtained through other ultrafast coherent spectroscopies. (c) Fourier Transform of the oscillating residuals highlighting the frequency components contributing to the beating. The data in panels (b) and (c) refer to sample measurements performed on HITCI dye solutions.

Despite the recognized importance of extracting also dynamical information, the current analysis techniques are based on Fourier transform analysis, providing only spectral information [Fig. 1(c)]. The idea of explicitly considering also the time dimension naturally leads to the concept of time-frequency and its representations. In signal processing, time–frequency analysis comprises all those techniques that study a signal in both the time and frequency domains *simultaneously,* using various time–frequency representations. Rather than independently considering the 1-dimensional representation of the signal in the time and frequency domains, *s(t)* and *S(v)*, respectively, the time–frequency analysis studies a two-dimensional signal *S(t,v)* spreading out the information content along the two dimensions of the time-frequency plane [Fig. 2].

Given their generality, time-frequency transforms (TFT) have found applications in several fields, from the interpretation of geophysics phenomena [15], to physiological responses [16], to radio- and tele-communications [17, 18] and their use has been intensified in particular in the last two decades. If the intensification of their use had the beneficial effect of providing the user with new and increasingly sophisticated tools, their development in fields often very different gave rise to an anthology of different developments that sometime makes quite difficult their actual use for specific applications.

The main objective of this paper is to present the main time-frequency methods available today and apply them specifically to oscillating signals obtained through (multidimensional) coherent spectroscopy. The application of time-frequency techniques, well established in other fields, is instead still poorly developed in spectroscopy. Indeed, apart from the pioneering works of T. Kobayashi and A. Stolow, who have demonstrated TFTs in analyzing wavepacket dynamics in ultrafast pump-probe signals, few are the examples of TFT analysis applied to spectroscopic signals. In particular the sliding-window Fourier Transform (or short-time Fourier transform as defined in Section 3.1) was successfully applied, for example, toward analysis of complex wavepacket dynamics in the gas-phase [19], dynamical mode

#240965 Received 14 May 2015; revised 23 Jun 2015; accepted 26 Jun 2015; published 17 Jul 2015

coupling and mode-mixing [20, 21], and real-time reaction dynamics in the condensed phase [22, 23].

The reader must anyway be aware that the possibility of retaining information both in time and in frequency domain cannot be achieved at any costs. Indeed, transforms are subject to the time-frequency uncertainty principle and thus it is not possible to reach simultaneously ideal resolution along both dimensions. Moreover, the possibility of maintaining the joint information across the time-frequency plane often leads to artifacts or aberrations whose importance depends on the nature of the signal and on the particular TFT employed. It is thus of pivotal importance to know the characteristics of the different available TFTs to select from time to time the approach and the parameters most suitable for the specific input signal to be analyzed and for the specific expected output.

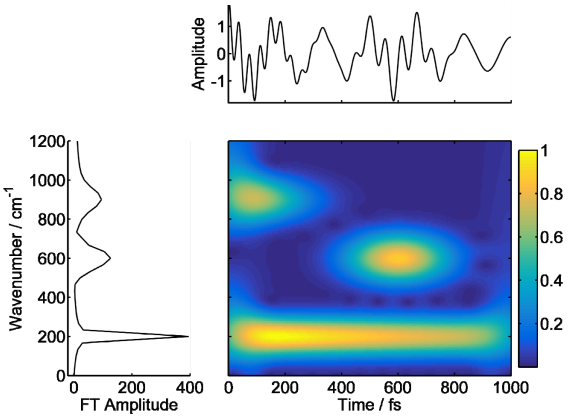

Fig. 2. Representation of the time-frequency plane. The 2D plot shows an example of a time-frequency map displaying the amplitude of signals at different frequencies over time, making it possible to track changes in amplitudes over a given time span. The originating signal is shown for comparison in the frequency and time domain on the left and on top, respectively.

2. Time-frequency transforms: definition and classification

Given a multi-component non stationary oscillatory signal, the associated time-domain representation *s(t)* and the frequency domain representation *S(v)* are related through the Fourier transform (FT):

$$S(\nu) = FT\{s(t)\} = \int_{-\infty}^{+\infty} s(t)\, e^{-i2\pi\nu t}\, dt \qquad (1)$$

The standard Fourier analysis plays an important role in signal processing, because it allows the decomposition of a signal into individual frequency components and establishes the relative intensity of each component. Often, the square of the FT (the power spectrum) is also used. In a conventional FT analysis, *S(v)* can be interpreted as the frequency representation of the signal as averaged over the entire time domain, and thus all the dynamical information is averaged over. It is therefore clear that the classical FT analysis is unsuitable for characterizing signals that only last for a short time or whose frequency contents change over time, situations that often happen in ultrafast spectroscopy signals. The representations in terms of time-frequency distributions overcome this limitation.

Several approaches have been followed historically for the formulation of time-frequency representations (TFT). The most known and diffused are those inspired by Fourier analysis. Other methods are based on a signal-dependent approach (e.g. using models assuming *a priori* the knowledge of the possible structure of the analyzed signals). Sometimes these two classes are referred in the literature as ‘traditional’ and ‘modern’, or ‘non parametric’ and

#240965 Received 14 May 2015; revised 23 Jun 2015; accepted 26 Jun 2015; published 17 Jul 2015

'parametric', respectively [24, 25]. Only TFTs belonging to the former group will be considered in this work.

Among them, a fundamental property is the dependence of the representation on powers of the signal *s(t)*. Here, only linear and bilinear TFTs, depending linearly and quadratically on the signal, respectively, will be analyzed. Higher order TFTs are also known but in general they are more difficult to apply and understand. The most known TFTs belong to the so-called Cohen's class [26]. Among them, the attention has been focused in particular on the short-time Fourier transform (STFT), the Margenau-Hill-Spectrogram distribution (MH), the Wigner-Ville distribution (WV), the Choi-Williams (CW) distribution, which present the most suitable properties for the application to spectroscopic signals. For a complete overview of the Cohen's class functions see for example [27–29].

3. Linear time-frequency transforms

3.1 Short-time Fourier transform (STFT)

The best-known linear time frequency representation dates back to Gabor [30] and is known as short-time Fourier transform (STFT). It examines the frequency content of the signal as a window is moved in time, providing the Fourier transform only of the portion of the signal contained in the window. The definition is straightforward:

$$STFT(t,\nu) = \int_{-\infty}^{+\infty} s(t')\, h^*(t'-t) e^{-i2\pi\nu t'}\, dt \qquad (2)$$

This operation differs from the FT only by the presence of the window *h(t)* centered at the time *t*. A well-know drawback of the STFT is the resolution limit imposed by the window function: a short time window provides better time resolution but more uncertainty in the frequency domain. Moreover, only those frequency components characterized by a time behavior comparable with the time amplitude of *h* will be properly characterized [Fig. 3].

Since in STFT the width of the window *h* is constant, the time-frequency resolution is fixed, and thus this is not the best approach to analyze multiscale signals with spread frequency contents, as typically obtained in a ultrafast coherent technique.

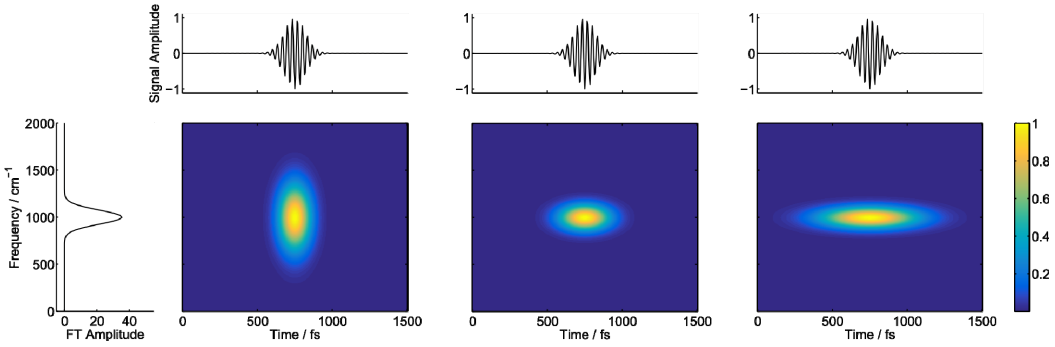

Fig. 3. Time-frequency plots showing the results of the analysis performed by STFT with Gaussian windows of increasing width from left to right. The original signal in the frequency and time domain is shown for comparison on the left and on top of the panels, respectively. The time resolution worsens from left to right.

3.2 Continuous wavelet transform (CWT)

A more advanced approach is represented by the continuous wavelet transform (CWT), not belonging to the Cohen's class, defined as:

#240965 Received 14 May 2015; revised 23 Jun 2015; accepted 26 Jun 2015; published 17 Jul 2015

$$CWT(t,a) = \frac{1}{\sqrt{|a|}} \int_{-\infty}^{+\infty} s(t')\,\psi^*\left(\frac{t'-t}{a}\right) dt \tag{3}$$

Here, instead than a fixed window *h(t)*, a short time oscillating function ψ, called 'wavelet' is used, where $a = v/v_0$ is the scale parameter that acts as a pseudo frequency and v_0 is the central frequency of the wavelet. The parameter a stretches the wavelet ψ as it is translated along time, leading to a variable resolution. The resulting signal at each time t will be higher if the typical frequencies of the signal match the frequency scale a of the wavelet. A distribution is then reconstructed, in which the signals show which wavelet scale contributes more to the wavelet decomposition at a given time. More details about the applications of wavelet transform to spectroscopic signals can be found in [31]. This approach is certainly more versatile to probe multiscale frequencies with respect to STFT. Nevertheless, a known drawback of wavelet decomposition is that, being the resolution frequency dependent, higher frequencies components are typically well resolved in time but less characterized in frequency.

4. Bilinear time-frequency transforms

The linear representations STFT and CWT perform a sort of 'localized' Fourier transform since they rely on the analysis of the oscillations in a limited time window (h or ψ) that is translated along the whole time axis. In both cases this implies limitations in the time-frequency resolution. Some of the bilinear TFTs overcome this limitation since they are able to distribute in a more sophisticated way the energy of the signal over the time-frequency plane. The simplest bilinear TFTs are obtained taking the square modulus of linear STFT and CWT, indicated with $|\mathrm{CWT}|^2$, $|\mathrm{STFT}|^2$, and referred often as scalogram and spectrogram, respectively. Here the quadratic dependence on the signal is trivial and does not add any peculiar characteristic to the already defined linear counterparts.

The strength of a bilinear approach in the time frequency analysis can be appreciated considering the Margenau-Hill-Spectrogram distribution [32], a modified version of the original Margenau-Hill distribution [33]. This simple transform can be expressed as the real part of the product between two different STFT having different time windows h and g:

$$MHS(t,v) = \mathrm{Re}\left\{STFT_h(t,v)\cdot STFT_g^*(t,v)\right\} \tag{4}$$

For practical purposes, the use of two different windows improves the resolution with respect to the squared modulus of the STFT, since the two windows can be independently chosen to adequately guarantee frequency and time resolution. The main drawback is however the possible generation of artifacts, arising when the window lengths are very different and the signal contains components with similar frequency.

A more advanced definition is introduced in the Wigner-Ville distribution (WV), one of the most diffuse and powerful bilinear time-frequency representations [34, 35]:

$$WV(t,v) = \int_{-\infty}^{+\infty} dt'\, s\left(t+\frac{t'}{2}\right) s^*\left(t-\frac{t'}{2}\right) e^{-i2\pi v t'} \tag{5}$$

In Eq. (5) the signal appears two times and is used in the form of analytic associate, i.e. the imaginary component of the complex signal s^* is obtained from the Hilbert transform of the real component s. The Wigner–Ville is the Fourier transform of the signal's autocorrelation function with respect to the delay variable. It can be thought of as a short-time Fourier transform where the windowing function is a time-scaled, time-reversed copy of the original signal.

The WV has a number of desirable properties for our purposes. First of all, the WV of any signal is always real and that it satisfies the so-called 'time and frequency marginal conditions' [36]: the integration of the distribution over the frequency gives the square modulus of the signal, $|s(t)|^2$, and the integration over the time gives the energy spectrum,

#240965 Received 14 May 2015; revised 23 Jun 2015; accepted 26 Jun 2015; published 17 Jul 2015

$|S(v)|^2$. In general the WV is characterized by good resolution that makes it one of the most exploited TFT in signal processing. However, a known drawback is the appearance of strong cross-term interference in the analysis of multicomponent signals [26]. The cross-term interference is manifested as oscillating features arising in the time-frequency plane halfway between each pairs of components [Fig. 4(a)].

One of the possible approaches to overcome this aberration is to multiply the integrand in Eq. (5) by two time windows g and h that are translated along the time dimension, like in the smoothed-pseudo-Wigner-Ville distribution (SPWV) [37]:

$$SPWV(t,v) = \int_{-\infty}^{+\infty} h(t') \int_{-\infty}^{+\infty} g(t''-t)\, s\left(t''+\frac{t'}{2}\right) s^*\left(t''-\frac{t'}{2}\right) e^{-i2\pi v t'}\, dt'\, dt'' \qquad (6)$$

From the practical point of view, SPWV provides good results even in the presence of many components and it contains little to none cross-term artifacts [Fig. 4]. However, because of the two time windows, the resolution is lower with respect to the original WV and the fulfillment of the marginal conditions become less rigorous.

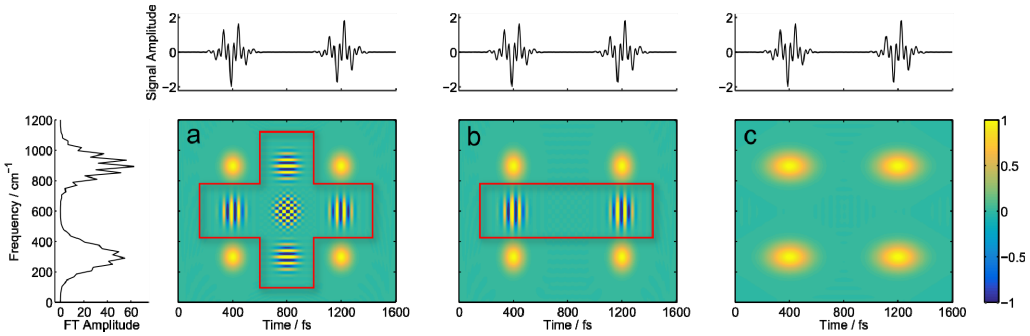

Fig. 4. Comparison between (a) Wigner-Ville [WV], (b) pseudo-Wigner-Ville [PWV] and (c) smoothed-pseudo-Wigner-Ville [SPWV] transforms. The original signal in the frequency and time domain is shown for comparison on the left and on top of the panels, respectively. Cross-term interference artifacts appearing between relevant signals along the time and frequency axes are highlighted by red lines. The introduction of the first window h removes interference between signals not superimposed in time. The second window g performs a smoothing in time, removing the residual interferences. The final SPWV does not present cross-terms contaminations but the resolution is clearly lowered.

In addition to the Margeneau-Hill-Spectrogram and the Wigner-Ville distribution and its derivatives, the Choi-Williams (CW) distribution [38] represents one of the best-known transforms of the Cohen's class. The CW distribution is defined as:

$$CW(t,v) = \int_{-\infty}^{+\infty} \int \frac{\sqrt{\alpha}}{\sqrt{4\pi}\,|t''|} \exp\left(-\frac{t'^2\,\alpha}{(4t'')^2}\right) s\left(t+t'+\frac{t''}{2}\right) s^*\left(t+t'-\frac{t''}{2}\right) e^{-i2\pi v t'} dt'\, dt'' \quad (7)$$

and it critically depends on the α parameter, introduced to solve the cross-term interference problem. When $\alpha \to \infty$ the WV distribution [Eq. (5)] is retrieved. The smaller the α parameter, the more effective is the reduction of the interference. Values of α too small may anyway leads to an overall degradation of the TFT map's content. A disadvantage of the CW distribution is that, although a good frequency resolution is obtained, it preserves strong interferences for synchronized components in time, manifested as deformations along the vertical axis. To overcome this limit, the same strategy used to obtain the SPVW from the WV can be adopted and the integrand in Eq. (7) can be multiplied by two time windows g and h, obtaining the smoothed Choi-Williams (SCW):

#240965 Received 14 May 2015; revised 23 Jun 2015; accepted 26 Jun 2015; published 17 Jul 2015

$$SCW(t,v)=\int_{-\infty}^{+\infty}h(t'')\int_{-\infty}^{+\infty}g(t')\frac{\sqrt{\alpha}}{\sqrt{4\pi}|t''|}\exp\left(-\frac{(t')^2\alpha}{(4t'')^2}\right)s\left(t+t'+\frac{t''}{2}\right)s^*\left(t+t'-\frac{t''}{2}\right)e^{-i2\pi vt''}dt'\,dt'' \tag{8}$$

5. Comparison of the performances of different transforms

For better understanding the performances of the discussed TFTs when applied to spectroscopic signals, they have been applied to the analysis of a synthetic signal *y(t)* constructed summing sinusoid waves with different frequencies and time dependent amplitudes:

$$y(t,v)=\sum_{n=1}^{3}A_n\exp(-t/t_n)\cos(2\pi v_n t) \tag{9}$$

The benefit of using a synthetic signal with known properties is that it is possible to judge the performances of the different TFTs simply comparing their results with the original frequencies and amplitudes. This is of course not trivial with real experimental data.

In this paper the discussion is limited for simplicity to 1D signals described as in Eq. (9), but the generalization to 2D signals is straightforward. The 1D signals analyzed here can indeed be interpreted as single decay traces extracted at specific (*x,y*) coordinates of the 2D map, as shown in Fig. 1.

There are several factors that may contribute to the final overall performances of a TFT analysis: (1) the nature of the input signal. Different TFTs may be more or less suitable towards the analysis of signals characterized by different frequencies and dynamics and may be more or less robust against noise. (2) The choice of the function used to describe the *g* and *h* windows and (3) the parameters on which these functions depend. The attempt to fully explore all the possible scenarios is not an easy task and goes beyond the scope of this paper. The aim here is not to identify the 'best' transform but bring attention to the power of time-resolved frequency analysis of multi-component oscillatory features in time-resolved spectroscopic measurements (including 2DES) as well as to provide the interested reader with a useful "guide" of possible approaches, highlighting their general advantages and drawbacks.

For this reason we first limit the discussion to a single example, shown in Fig. 5, used to illustrate the different circumstances and artifacts that may typically appear during the analysis with the considered TFTs. In this example the values of the frequency and time parameters adopted to generate the signal shown in Fig. 5(a) have been chosen in order to mimic the values typically encountered in experiments. To obtain a meaningful comparison, a Gaussian function was chosen to represent the *g* and *h* windows for all the analyzed TFTs. For each transform, the windows parameters have been chosen to provide an optimized matching with the originating signal. The final results are summarized in Fig. 5(b)-5(f).

Figure 5 clearly highlights the major advantages and drawbacks of the different approaches. For example, the frequency dependent resolution of CWT commented in section 3.2 is clearly recognizable in panel (b), where the higher frequency components of the signal are very poorly resolved. The scalogram ($|CWT|^2$, panel b), the spectrogram, ($|STFT|^2$, panel c) and the Margenau-Hill spectrogram (MHS, panel d) show similar deformations of the signals along the time dimension, manifested as aberrations close to the limits of the investigated time window (at *t*~0 and *t*~600fs). The three frequency components seem indeed to reach a maximum amplitude at time>0, instead that showing the expected exponentially decreasing behavior. This deviation may complicate a lot the interpretation of the dynamics of real signals. The smoothed-pseudo-Wigner-Ville (SPWV, panel e) and the smoothed Choi-Williams (SCW, panel f) are instead characterized by a good resolution and accuracy both along the time and the frequency axes. The SCW, despite the good resolution achieved, shows vertical artifacts typical of such approach.

#240965 Received 14 May 2015; revised 23 Jun 2015; accepted 26 Jun 2015; published 17 Jul 2015

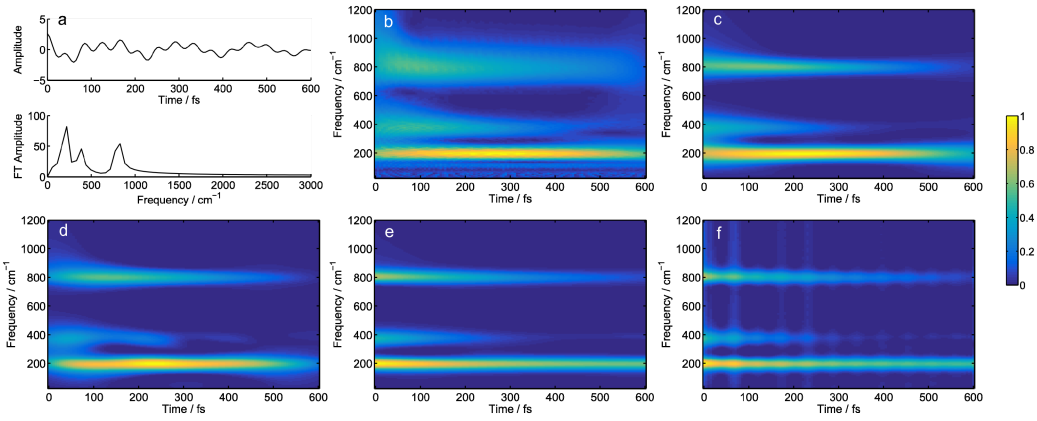

Fig. 5. Comparison of the results obtained applying different TFT analysis to a multicomponent signal mimicking experimental data. (a) Analyzed signal in the time and frequency domain. In this specific case: ν_1 = 200cm^{-1}; ν_2 = 375cm^{-1}; ν_3 = 800cm^{-1}; t_1 = 2ps; t_2 = 200fs ; t_3 = 500fs; $A_1 = A_2 = A_3 = 1$; (b) Scalogram (|CWT|^2), obtained with a gaussian Morlet window $\psi = (1/\sigma_b\sqrt{2\pi})\exp(-t/2\sigma_b)^2 \cdot \exp(i2\pi f_c t)$ with σ_b = 0.7 and f_c = 1; (c) Spectrogram, (|STFT|^2), Gaussian window $h(t) = (1/\sigma_h\sqrt{2\pi})\exp(-t^2/4\sigma_h)$ σ_h = 100 fs; (d) Margenau-Hill spectrogram (MHS), σ_h = 55 fs and σ_g = 150 fs; (e) Smoothed-pseudo-Wigner-Ville (SPWV), $\sigma_h = \sigma_g$ = 75 fs; and (f) Smoothed Choi-Williams (SCW), $\sigma_h = \sigma_g$ = 80 fs, α = 0.1.

5.1 Exploring TFT performances as a function of the signal properties

The performances of the considered TFTs have been tested also for a wider range of signals. We have analyzed signals characterized by frequencies ν_n spanning the typical range of experimental oscillations recorded in ultrashort broadband (2D) electronic spectroscopy (100-1500 cm^{-1}) and characterized by dephasing times t_n much shorter and/or much longer than the maximum delay time, in order to explore all the possible scenarios with respect to the FT frequency resolution.

Except for the scalogram (|CWT|^2), which presents by definition a frequency-dependent resolution, the other transforms did not reveal particular differences in the performances when applied to different signals. A general behavior, common to all transforms, is the difficulty in analyzing signals characterized by low frequencies and short dephasing times (with respect to the overall time range considered). In this situation only few periods of the oscillation are available and thus the uncertainty in the analysis may be high.

5.2 Noise effects

Since experimental measures may be affected by large amount of noise, it is important to test how the transforms behave in the presence of various noise levels. The performances of the TFTs have been calculated for a series of signals defined as $y_{noise}(t) = y(t) + k \cdot n(t)$ where *n(t)* is a source of gaussian noise and *k* is a scaling factor. The calculations have been done for *k* = 0,1, 0.2, 0.5 and 1. Figure 6 shows the results obtained starting from the same signal *y(t)* used in Fig. 5 with *k* = 0.5.

The noise degrades the results of all transforms with about the same efficiency; as the level of noise increases, the number of artifacts along the frequency dimension increases giving rise to spurious signals especially at early times. In general the MHS (panel d) and the CW (panel f) seem to be less robust against noise, especially if compared with SPWV (panel e), which performs quite well even in the presence of relatively high levels of noise.

#240965 Received 14 May 2015; revised 23 Jun 2015; accepted 26 Jun 2015; published 17 Jul 2015

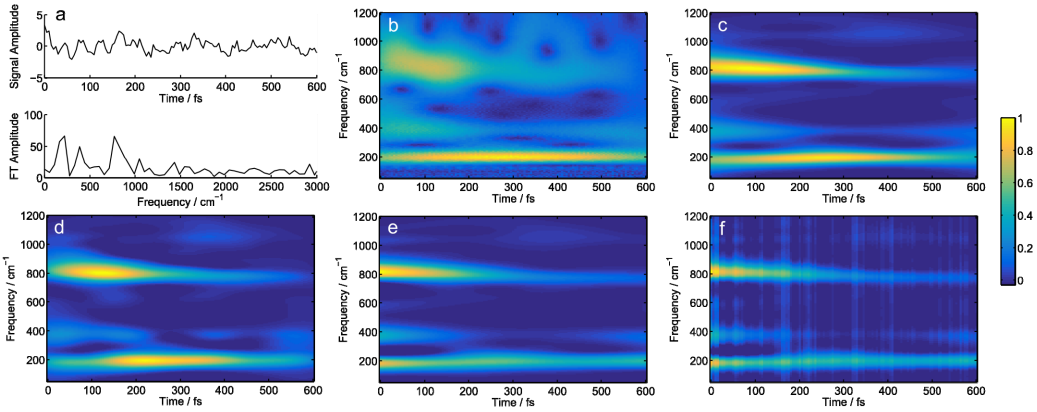

Fig. 6. Effect of the noise on TFT performances. (a) Analyzed signal in the time and frequency domain. In this specific case: $\nu_1 = 200\text{cm}^{-1}$; $\nu_2 = 375\text{cm}^{-1}$; $\nu_3 = 800\text{cm}^{-1}$; $t_1 = 2\text{ps}$; $t_2 = 200\text{fs}$; $t_3 = 500\text{fs}$; noise level $k = 0.5$. (b) Scalogram ($|\text{CWT}|^2$); (c) Spectrogram ($|\text{STFT}|^2$); (d) Margenau-Hill spectrogram (MHS); (e) Smoothed-pseudo-Wigner-Ville (SPWV); and (f) Smoothed Choi-Williams (SCW). Window parameters as in Fig. 5.

5.3 Choice of the window functions

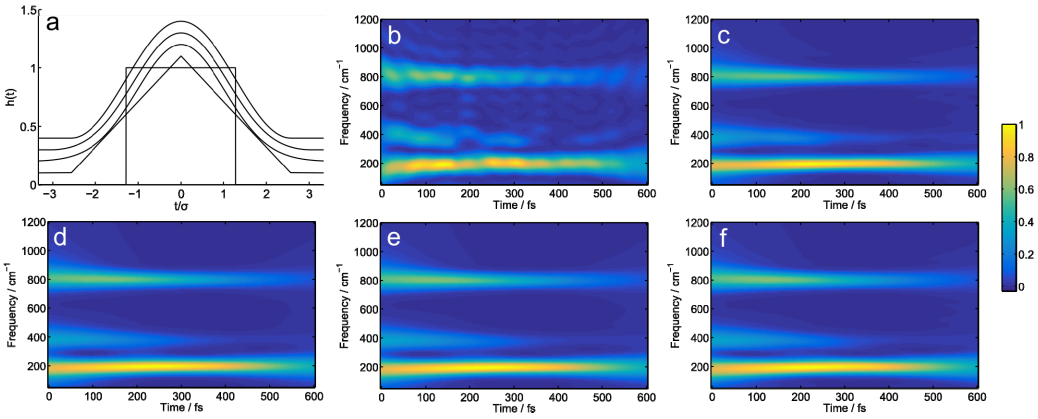

Fig. 7. (a) Windows functions tested in the TFT analysis. From the bottom to the top: top-hat, Bartlett, Gaussian, Blackman, and Hanning function. The windows have been normalized by area. (b-f) Results obtained applying the Short Time Fourier Transform (STFT) for the analysis of the signal of Fig. 5 using (b) the top-hat window function; (c) the Bartlett window function; (d) the Gaussian window function; (e) the Blackman window function, and (f) the Hanning window function.

To illustrate how the choice of the window function may affect the results of the TFT analysis, we repeated the calculations using several window shapes commonly used in time-frequency analysis. The results obtained for the STFT are reported in Fig. 7. Apart for the rectangular (top-hat) function generating the expected ringing artifacts (panel b), all the considered functions lead to similar results. Given this weak dependence on the window functions, Gaussians are often chosen for simplicity [39].

5.4 Optimization of the window parameters

While the shape of the window function has little effects on the performances of the TFTs, the choice of the window parameters is instead crucial to satisfactorily retrieve both time and frequency information. For example, for a Gaussian window written as

#240965 Received 14 May 2015; revised 23 Jun 2015; accepted 26 Jun 2015; published 17 Jul 2015

$G(t) = (1/2\pi\sigma^2)^{1/2} \cdot \exp[-(t/2\sigma)^2]$, the balance about time and frequency resolution is controlled by the parameter σ: the bigger the value of σ, the narrower the frequency bandwidth (longer time duration), and *vice versa*.

Each transform responds in a different way to the variation of the windows parameters, as expected considering their different mathematical definitions. General trends are difficult to identify, being the final result also dependent on the analyzed signal. In general it is observed that windows characterized by smaller width in time guarantee better time resolution but frequency information is degraded. σ must thus be carefully chosen to obtain a good compromise between frequency and time resolution. The choice is necessarily application-dependent and depends on the information one wants to retrieve.

6. Remarks and conclusions

In the latest years, experimental 2DES experiments are producing a growing amount of evidences proving the crucial role of the interplay between vibrational and electronic coherences in the dynamics of transport processes, manifested as multicomponent non-stationary oscillating signals. Conventional Fourier Transform analysis is not suitable for a thorough characterization of such signals where different components can last for short times and whose frequency contents change over time. Time-frequency analysis methods, able to spread the signal information along both the time and frequency domains *simultaneously,* are thus particularly promising but they have not yet been significantly applied to the analysis of spectroscopic signals.

In this work, several time-frequency transforms, borrowed from the signal-processing field, have been reviewed and applied to the investigation of signals from multidimensional coherent electronic spectroscopy. Advantages and drawbacks of each approach were fully investigated and possible artifacts and source of mistakes have been highlighted.

The emerging picture is that, on one side, these methods are extremely powerful in extracting higher-level information about the energetics and the dynamics of coherence superposition of states; on the other side, the time-frequency uncertainty principle that naturally limits this treatment, makes it also particularly prone to artifacts, easily mistaken by real features. How easy it is to distinguish artifacts from real signals depends on the characteristics of the signal itself and thus the operator has to select from time to time the TFT and the parameters most suitable for the specific input signal to be analyzed and for the specific expected output. We hope that this manuscript may help the interested reader in such a task.

Acknowledgments

This work is supported by the ERC Starting Grant QUENTRHEL (278560), FP7 FET EC project MULTI (317707) and FP7 EU STREP project PAPETS (323901).

#240965 Received 14 May 2015; revised 23 Jun 2015; accepted 26 Jun 2015; published 17 Jul 2015